Domain wall dynamics and Barkhausen effect in metallic ferromagnetic materials. II. Experiments

# Domain-wall dynamics and Barkhausen effect in metallic ferromagnetic materials. II. Experiments

Bruno Alessandro, Cinzia Beatrice, Giorgio Bertotti, and Arianna Montorsi

Citation: Journal of Applied Physics **68**, 2908 (1990); doi: 10.1063/1.346424
View online: http://dx.doi.org/10.1063/1.346424
View Table of Contents: http://scitation.aip.org/content/aip/journal/jap/68/6?ver=pdfcov
Published by the AIP Publishing



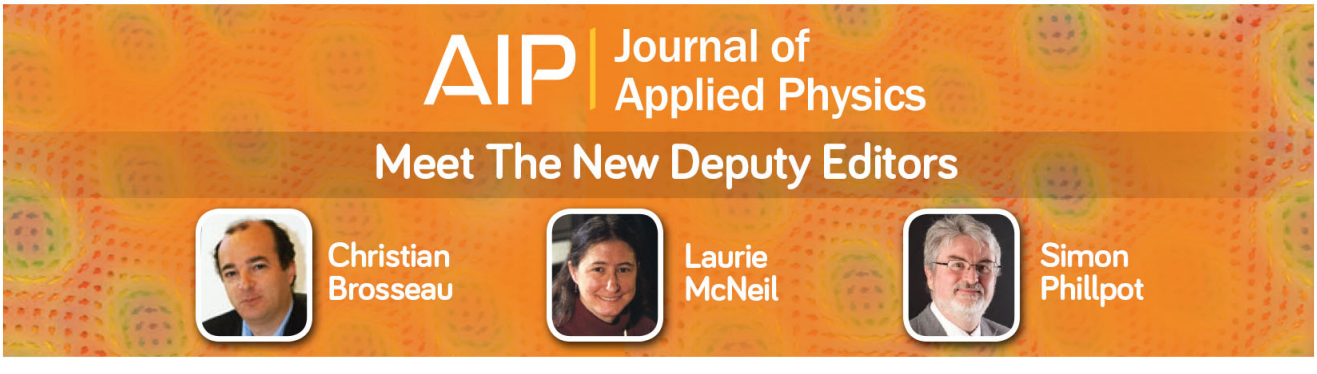

# Domain-wall dynamics and Barkhausen effect in metallic ferromagnetic materials. II. Experiments

Bruno Alessandro,[a] Cinzia Beatrice, Giorgio Bertotti, and Arianna Montorsi[b]
*Istituto Elettrotecnico Nazionale Galileo Ferraris and Centro Interuniversitario Struttura della Materia, C. M. d'Azeglio 42, I-10125 Torino, Italy*

(Received 9 February 1990; accepted for publication 4 May 1990)

Barkhausen effect (BE) phenomenology in iron-based ferromagnetic alloys is investigated by a proper experimental method, in which BE experiments are restricted to the central part of the hysteresis loop, and the amplitude probability distribution, $P_0(\dot{\Phi})$, and power spectrum, $F(\omega)$, of the $B$ flux rate $\dot{\Phi}$ are measured under controlled values of the magnetization rate $\dot{I}$ and differential permeability $\mu$. It is found that all of the experimental data are approximately consistent with the law $P_0(\dot{\Phi}) \propto \dot{\Phi}^{\tilde{c}-1} \exp(-\tilde{c}\dot{\Phi}/\langle\dot{\Phi}\rangle)$, where all dependencies on $\dot{I}$ and $\mu$ are described by the single dimensionless parameter $\tilde{c}>0$. Also the parameters describing the shape of $F(\omega)$ are found to obey remarkably simple and general laws of dependence on $\dot{I}$ and $\mu$. The experimental results are interpreted by means of the Langevin theory of domain-wall dynamics proposed in a companion paper. The theory is in good agreement with experiments, and permits one to reduce the basic aspects of BE phenomenology to the behavior of two parameters describing the stochastic fluctuations of the local coercive field experienced by a moving domain wall.

## I. INTRODUCTION

The Barkhausen effect[1-7] (BE) is easily detectable by means of a pickup coil wound around a ferromagnetic specimen, when the material is magnetized under the action of a varying external field $H_a$. The induced voltage exhibits stochastic fluctuations ($B$ noise) which, at low magnetization rates, result in large bursts (commonly termed $B$ pulses or $B$ jumps) separated by random waiting times. It is well known that this behavior originates from the random nature of the interactions of magnetic domain walls (DWs) among themselves and with microstructural defects (impurities, dislocations, grain boundaries, etc.). Loosely speaking, the value of the BE flux rate per coil turn, $\dot{\Phi}$, measures the velocity of active DWs and a $B$ jump indicates a sudden passage of the magnetic domain structure to a new metastable configuration. In this respect, BE is a most sensitive probe and represents, in principle, a powerful, unique tool to study the processes at the origin of ferromagnetic hysteresis.

However, the translation of this general statement into a quantitative experimental approach is by no means a simple task, owing to the inherent complexity of BE phenomenology. In fact, BE statistical properties show a highly nontrivial, nonlinear dependence on demagnetizing effects (i.e., on the apparent permeability of the system), as well as on the magnetization rate of change $\dot{I}$. Several authors have stressed the presence and the puzzling character of these nonlinearities when BE fluctuations of low angular frequency $\omega$ (say $\omega/2\pi \lesssim 10^2$ Hz) are considered.[2,8,9] On the other hand, BE properties are strongly dependent on the point of the hysteresis loop where they are considered. Of course, this may be the consequence of the use, as is often the case, of a triangular applied field waveform, which produces a magnetization rate $\dot{I}$ proportional to the differential permeability[10] $\mu = dI/dH_a$. This complication, however, can be avoided by modifying the field waveform, in order to obtain a constant $\dot{I}$ along each half-loop.[11] But even when this is done, BE does not exhibit stationary properties in the half-loop. The reason is that magnetostatic effects, measured by $\mu$, change along the loop, thus affecting the $B$ noise behavior. In addition, domain creation and annihilation processes contribute to BE only when the magnetization approaches the saturation value, but not in the central part of the loop, around $I \sim 0$, where DW motion is the dominant process. BE investigations which do not take these aspects into account, and average BE properties over the whole hysteresis loop, will inevitably confuse the effects of different magnetization mechanisms and different dynamic conditions (measured by $\dot{I}$ and $\mu$) in an intricate way, thus hindering an adequate physical interpretation.

In the present paper, we discuss an experimental approach[12] where these difficulties are avoided by limiting BE measurements to a narrow magnetization interval $\Delta I$ of each hysteresis half-loop, centered around $I=0$, where $\mu$ is usually fairly constant. An external field increasing at a constant rate $\dot{H}_a$ produces, in this interval, a constant magnetization rate $\dot{I} = \mu\dot{H}_a$. The BE signal corresponding to $\Delta I$ has, in each half-loop, a duration $\Delta t = \Delta I/\dot{I}$, and within this time interval it is expected to behave as a stationary stochastic process, associated with the well-defined magnetization mechanism, DW motion, and with well-defined values of $\dot{I}$ and $\mu$. These values are controlled by the frequency of the applied field waveform and the degree of magnetic flux closure at the ends of the specimen. They can be varied over a

[a] Present address: Istituto Nazionale di Fisica Nucleare Sezione di Torino, I-10125 Torino, Italy.
[b] Also Dipartimento di Fisica, Politecnico di Torino, I-10124 Torino, Italy.

 0021-8979/90/182908-08$03.00  

wide range in order to explore the dependence on $\dot{I}$ and $\mu$ of the two quantities which provide the basic statistical characterization of the $B$ signal, i.e., the amplitude probability distribution $P_0(\dot{\Phi})$ and the power spectrum $F(\omega)$ of the BE flux rate $\dot{\Phi}$.

By this method, we have carried out a comprehensive investigation of BE behavior as a function of $\dot{I}$ and $\mu$ in polycrystalline 3% SiFe over the range $2.5\times10^3<\mu/\mu_0<6\times10^4$ and $1.5\times10^{-4}\ \mathrm{T\,s^{-1}}<\dot{I}<1.5\ \mathrm{T\,s^{-1}}$. Our experiments show that the dependence of $P_0(\dot{\Phi})$ and $F(\omega)$ on $\dot{I}$ and $\mu$ is governed by remarkably simple and general laws. To a good degree of approximation, all of the experimental data are in agreement with the law

$$P_0(\dot{\Phi}) = k_P \dot{\Phi}^{\tilde{c}-1} \exp(-\tilde{c}\dot{\Phi}/S\dot{I}), \tag{1}$$

where $k_P$ is a normalization constant, $S$ is the specimen cross-sectional area, and the dependencies on $\dot{I}$ and $\mu$ are included in the parameter $\tilde{c}>0$. As regards the BE power spectrum $F(\omega)$, we have found that $F(\omega)$ exhibits a maximum

$$F_M = S\dot{I}g_F(\dot{I})(\mu/\mu_0)^{3/2} \tag{2}$$

at the frequency $\omega_M \propto \dot{I}^{1/2}$, where the function $g_F(\dot{I})$ being fairly constant over a wide $\dot{I}$ range. When $\omega \gg \omega_M$, $F(\omega)$ approaches the law

$$F(\omega) \simeq k_F \dot{I}/\omega^2, \tag{3}$$

where $k_F$ is independent of $\dot{I}$ and $\mu$.

These laws are the basic result of our studies. They provide a clear, quantitative description of BE phenomenology, and a stringent test of theoretical models. In this connection, we will compare them with the predictions of the Langevin description of DW motion proposed in the preceding companion paper.[13] The dependence of BE properties on $\dot{I}$ and $\mu$ is satisfactorily reproduced by the theory, under quite natural and reasonable assumptions about the parameters that describe the DW interaction with the surrounding perturbed medium. It must be stressed that direct physical conclusions can be drawn from this comparison basically because the assumptions made in the theory (that DW motion is the relevant magnetization mechanism and that BE can be described as a stationary stochastic process, associated with well-defined values of $\dot{I}$ and $\mu$) have a precise counterpart in the conditions under which the experiments are carried out.

We conclude with a comment on the generality of the results presented in this paper. In our opinion, they are representative of BE behavior in a wide class of metallic ferromagnetic materials. The literature gives strong support to this statement. The shape of the BE power spectrum $F(\omega)$ found in the present experiments is basically the same, within a scale factor, as in NiFe alloys with vanishing anisotropies,[14] in grain-oriented 3% SiFe alloys with Goss or cubic texture,[11] and in 3% SiFe single crystals.[15] The law $F_M \propto \mu^{3/2}$ has been found for fixed $\dot{I}$ in experiments on SiFe single crystals,[15] and is also indirectly supported by other experiments[2] on grain-oriented 3% SiFe. The high-frequency law $F(\omega) \simeq k_F \dot{I}/\omega^2$, which holds even when the $B$ noise is averaged over the whole hysteresis loop, has been known for a long time.[16] This generality of BE properties appears even more remarkable when it is contrasted with the extreme variety of the magnetic domain structures present in NiFe (the very existence and nature of DWs is debated), in SiFe polycrystals (an intricate domain pattern is present in each grain, with strong magnetostatic interactions from grain to grain), and in SiFe single crystals (a few antiparallel domains of macroscopic size, separated by 180° DWs are ordinarily the case). Certainly, with BE we are in the presence of a phenomenon of deep physical meaning, in direct connection with the basic principles governing ferromagnetic hysteresis.

## II. EXPERIMENT

Measurements were performed on a strip of nonoriented polycrystalline 3% SiFe (of grain size $\sim 100\,\mu$m) of dimensions $0.2\times0.01\times(3.5\times10^{-4})$ m, placed in a configuration shown schematically in Fig. 1. The experiment was included in a double-mumetal box, and all measurements were carried out in a shielded room in order to avoid spurious contributions to the detected signal. The strip was subjected to a slight tensile stress $\sim 5$ MPa. The magnetic circuit was closed by means of a mumetal yoke, separated from the strip by a variable nonmagnetic gap. By adjusting the gap width, it was possible to vary the differential permeability $\mu = dI/dH_a$ in the magnetization interval $\Delta I$ of interest from $\mu/\mu_0 = 2.5\times10^3$ (open strip) to $\mu/\mu_0 = 6\times10^4$ (yoke in contact with the strip). The strip was magnetized by applying a triangular current waveform to a solenoid. The magnetizing current frequency was varied so as to investigate various magnetization rates over the range $1.5\times10^{-4}\ \mathrm{T\,s^{-1}}<\dot{I}<1.5\ \mathrm{T\,s^{-1}}$. The peak magnetization $I_M$ of the hysteresis loop was kept equal to 1.3 T in all experiments. It was found that the BE behavior around $I=0$ did not change appreciably when considering loops with $I_M > 1.3$ T, so that we can simply describe the present experiments as referring to the saturation hysteresis loop of the material. On the other hand, we expect some dependence of BE on $I_M$, when $I_M \lesssim 1$ T. The investigation of this dependence, which should provide further insight into the connection between BE and magnetization processes, lies outside the scope of the present paper.

The $B$ noise was detected by a 50-turn coil, whose width was $\sim 2$ mm, that was placed in the middle of the strip. We stress the importance of using a narrow enough coil, which ensures that the induced voltage is proportional to the magnetic flux rate of change $\dot{\Phi}$ in a definite cross section. When

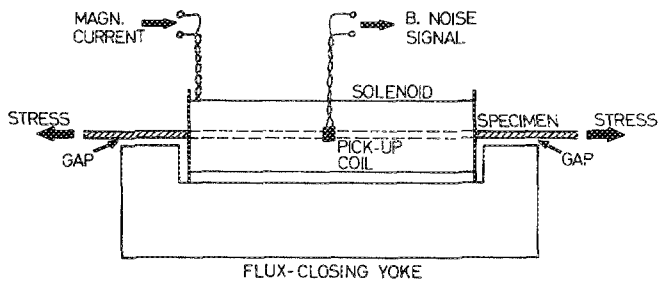


FIG. 1. Schematic representation of experimental setup.

wider coils, even covering the whole specimen, are employed, low-frequency noise fluctuations, which have a longer spatial correlation length,[5,17] are enhanced with respect to the high-frequency ones. The experiment then becomes dependent on the coil characteristics and the results are not easily amenable to a clear physical interpretation. The detected voltage was amplified by a low-noise, dc-coupled PAR 113 amplifier, and was processed by a Nicolet 660 analyzer. dc coupling is essential to obtain meaningful data on the amplitude probability distribution, $P_0(\dot{\Phi})$, especially at low $\dot{I}$, where $P_0(\dot{\Phi})$ exhibits a strongly non-Gaussian behavior. In power spectrum measurements, a careful subtraction of the amplifier background noise was performed. In this way, we were able to measure the noise spectrum down to 0.1 Hz even at the lowest magnetization rates ($1.5\times10^{-4}$ T s$^{-1}$) that were investigated.

As anticipated in the introduction, BE investigations were restricted to a central magnetization interval $\Delta I$ of each half-loop. In each experiment, several subsequent half-loops were considered in order to achieve a satisfactory statistical averaging of $P_0(\dot{\Phi})$ and $F(\omega)$. The interval $\Delta I$ was selected by means of a trigger circuit which, at controlled applied field levels, started and stopped the signal acquisition and analysis. The appropriate trigger field levels were chosen, case by case, by direct inspection of the behavior of the differential permeability along the half-loop, determined from the corresponding behavior of the magnetization rate at constant $\dot{H}_a$. An example of the typical permeability behavior is shown in Fig. 2. The plateau where $\mu$ is fairly constant is evident, and the interval where the noise analysis was carried out is indicated. It corresponds to a magnetization interval of 0.4 T. Actually, the choice $\Delta I = 0.4$ T was found to be appropriate for all the investigated $\mu$ values. Note that, by this method, the contribution of the periodic flux rate waveform to the signal processed by the analyzer is simply a constant, which is ignored in the Fourier analysis. Consequently, the power spectrum is not altered by the presence of lines related to periodic contributions to the signal and can be measured with good accuracy up to fairly high magnetization rates, $\dot{I} = 1.5$ T s$^{-1}$ in the present experiments. The main limitation of this method is that it can provide information only on BE fluctuations of frequency $\omega/2\pi \gtrsim \dot{I}/\Delta I$, and this lower bound of course increases with increasing $\dot{I}$.

## III. RESULTS ON AMPLITUDE PROBABILITY DISTRIBUTION

When considering BE statistical properties, in the past attention has often been focused on the signal autocorrelation function or the power spectrum. In fact, these quantities give direct information on the most striking and peculiar feature of BE, the clustering of magnetization reversals into large bursts. But important results can also be obtained from the amplitude probability distribution, $P_0(\dot{\Phi})$, measuring the probability that the $B$ flux rate per coil turn, $\dot{\Phi}$, attains a given value at a generic time. The study of this quantity is analogous to $B$ pulse counting experiments.[18–20] However, the results of these studies are weakened by the fact that the concept of single, separately detectable $B$ pulse applies only to low magnetization rates. On the other hand, the number of $B$ pulses, without consideration of their size, is often not a quantity of direct physical interpretation. $P_0(\dot{\Phi})$ is expected to provide the same type of information in a much better way.

The dependence of $P_0(\dot{\Phi})$ on $\dot{I}$ and $\mu$ was investigated by the method discussed in the previous section. A typical result of this study, referring to fixed $\mu$ and variable $\dot{I}$, is shown in Figs. 3 and 4, where semilogarithmic scales are used to make visible the details of the behavior of $P_0$ in the high $\dot{\Phi}$ tails. At high $\dot{I}$, $P_0(\dot{\Phi})$ tends to become a Gaussian of width definitely smaller than its mean value, $\langle\dot{\Phi}\rangle = S\dot{I}$. In terms of DW motion, this means that the DWs are moving at a velocity $v \propto \langle\dot{\Phi}\rangle$, and weakly fluctuating around this aver-

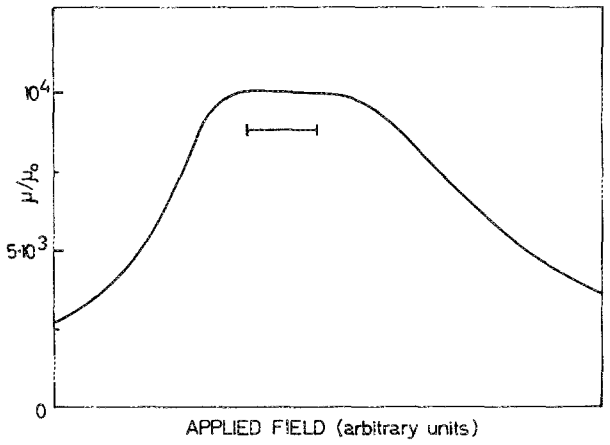


FIG. 2. Typical behavior of differential permeability along the hysteresis half-loop. The bar indicates the field interval where $B$ noise is analyzed. It corresponds to a magnetization interval of 0.4 T.

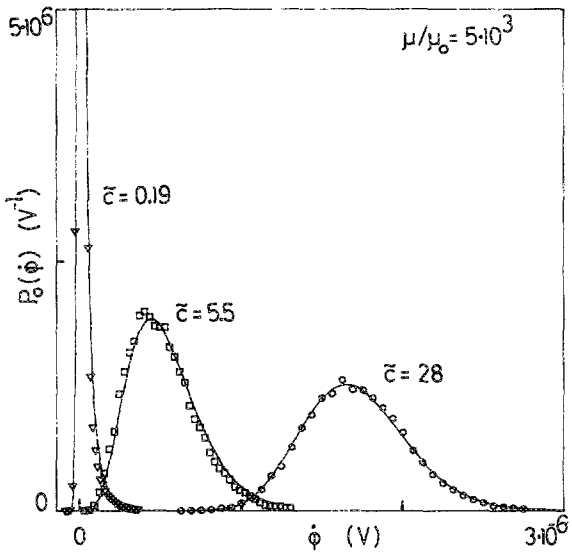


FIG. 3. Amplitude probability distribution $P_0(\dot{\Phi})$, measured at fixed permeability, $\mu/\mu_0 = 5\times10^3$, and variable $\dot{I}$: ($\nabla$) $4.9\times10^{-3}$ T s$^{-1}$; ($\square$) 0.15 T s$^{-1}$; ($\circ$) 0.49 T s$^{-1}$. Continuous lines are calculated from Eq. (1), using $\bar{c}$ values given in the figure.

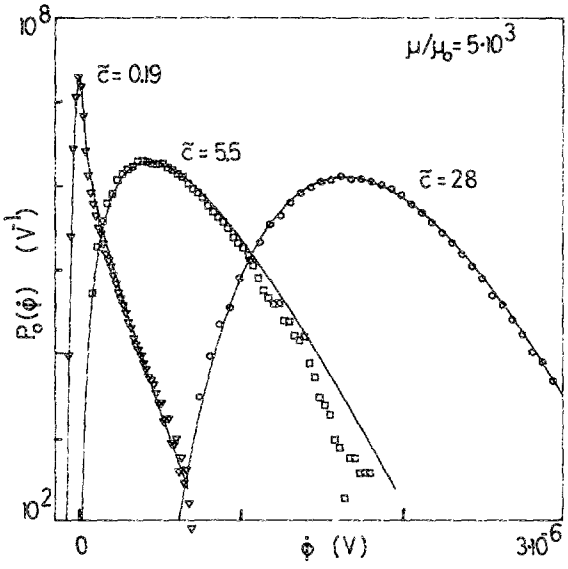


FIG. 4. Same as Fig. 3, represented in semilogarithmic scales.

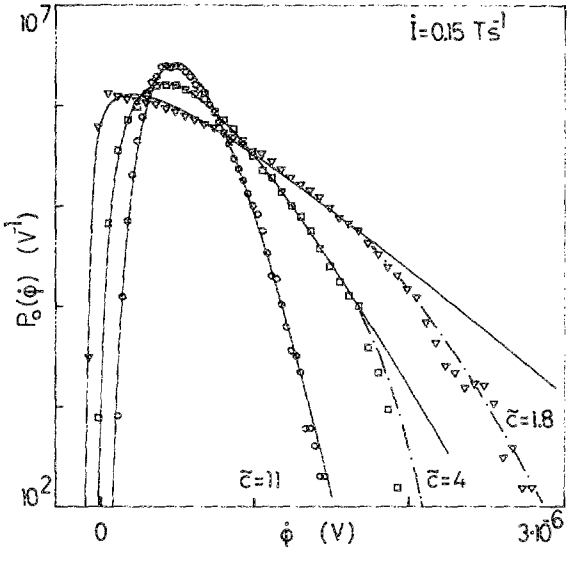


FIG. 5. Amplitude probability distribution $P_0(\dot{\Phi})$, measured at fixed magnetization rate, $\dot{I} = 0.15$ T s$^{-1}$, and variable $\mu/\mu_0$: (○) $2.5\times10^3$; (□) $10^4$; (▽) $6\times10^4$. Continuous lines are calculated from Eq. (1), using $\tilde{c}$ values given in the figure. Broken-dotted lines are obtained from computer simulations assuming $A = 1.65\times10^6$ A$^2$ m$^{-3}$ Wb$^{-1}$ and (□) $\xi = 8.4\times10^{-9}$ Wb, (▽) $\xi = 1.3\times10^{-8}$ Wb.

age value. With decreasing $\dot{I}$, $P_0(\dot{\Phi})$ progressively acquires a non-Gaussian shape and tends to diverge for $\dot{\Phi}\to0$, when $\dot{I}$ is sufficiently low. This behavior corresponds to the presence of $B$ bursts separated by finite time intervals where $\dot{\Phi}\sim0$. In other words, the DW motion becomes intermittent as a consequence of the hindering effect of pinning centers and DW-DW interactions.

As shown in Fig. 5, a similar behavior is observed when, instead of decreasing $\dot{I}$ at fixed $\mu$, we increase $\mu$ at fixed $\dot{I}$. In fact, it is known[15] that clustering phenomena in BE are destroyed by magnetostatic fields and are thus expected to be favored not only by a low magnetization rate, but also by a high permeability. The remarkable point is that this analogy is not merely qualitative, but can be given a definite quantitative form. Actually, we have found that all of our measurements could be fitted well by Eq. (1), where the dependencies on $\dot{I}$ and $\mu$ are included in the single dimensionless parameter $\tilde{c}>0$. According to Eq. (1), the behavior of $P_0(\dot{\Phi})$ for $\dot{\Phi}\to0$ changes drastically, from $P_0(\dot{\Phi})\to0$ to $P_0(\dot{\Phi})\to\infty$, when $\tilde{c}$ crosses the value $\tilde{c}=1$. We can say that $\tilde{c}=1$ defines the boundary between the regime ($\tilde{c}>1$) of continuous DW motion and that ($\tilde{c}<1$) of intermittent DW jumps. Note, however, that the divergence of $P_0(\dot{\Phi}\to0)$ when $\tilde{c}<1$ cannot be directly observable in experiments. In fact, assuming that Eq. (1) describes the BE amplitude distribution, the distribution actually measured in experiments will not correspond directly to Eq. (1), but to the convolution of Eq. (1) with the Gaussian distribution of the amplifier background noise. The latter can, however, be measured independently and the convolution calculated with no arbitrary parameters in addition to $\tilde{c}$. This was the procedure that was followed in the comparison between experiments and Eq. (1). A typical example of the agreement thus obtained is shown by the continuous lines in Figs. 3, 4, and 5.

The basic features of the dependence of $P_0(\dot{\Phi})$ on $\dot{I}$ and $\mu$ are reproduced by Eq. (1) rather comprehensively, but under specific conditions (low $\dot{I}$ and/or high $\mu$) a significant discrepancy is sometimes observed. The measured distribution decays to zero as $\exp(-\tilde{c}\dot{\Phi}/S\dot{I})$ only up to some maximum flux rate, beyond which a definitely stronger decay takes place, as shown in Fig. 5. In Sec. V, we will show that this behavior has a precise physical meaning, consistent with the Langevin description of DW dynamics proposed in paper I. In fact, Eq. (1) can be derived from this description under approximations which no longer hold for low $\dot{I}$ or high $\mu$. When the general theory, without approximations, is investigated by computer simulations, it is found that the behavior of $P_0(\dot{\Phi})$ predicted by the theory is always in good agreement with experiments. These numerical results have permitted us to determine the parameter $\tilde{c}$ in those cases where Eq. (1) led to ambiguous and unreliable fits.

Figure 6 summarizes our investigations on the BE amplitude probability distribution by showing the behavior of the parameter $\tilde{c}$ as a function of $\dot{I}$ for various $\mu$. The values determined directly through Eq. (1) are represented by the open symbols, while the filled symbols indicate those cases where the support of computer simulations was needed. To a good degree of approximation, $\tilde{c}\sim\dot{I}^{3/2}$ in the region $\tilde{c}>1$, and tends to $\tilde{c}\sim\dot{I}$ when $\tilde{c}<1$. The permeability dependence is approximately $\tilde{c}\sim\mu^{-1/2}$. The physical meaning of these results will be discussed in Sec. V.

## IV. RESULTS ON POWER SPECTRUM

We have applied the method discussed in Sec. II to study how the power spectrum $F(\omega)$ of the flux rate per coil turn, $\dot{\Phi}$, depends on $\dot{I}$ and $\mu$. Typical results are shown in Fig. 7 (variable $\dot{I}$ and fixed $\mu$) and Fig. 8 (variable $\mu$ and fixed $\dot{I}$). In analogy with amplitude distribution results, similar effects are observed when $\dot{I}$ is increased or $\mu$ is decreased. These modifications are characterized by few, remarkably

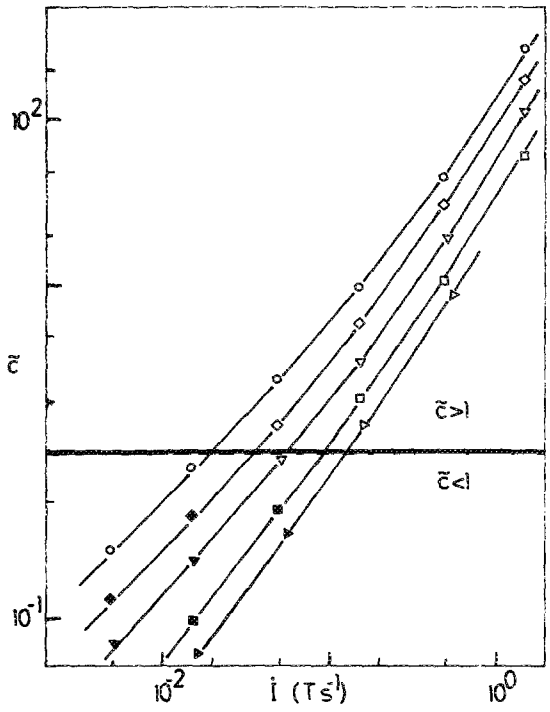


FIG. 6. Parameter $\tilde{c}$ of Eq. (1), obtained by fitting experimental data, vs $\dot{I}$ for different values of $\mu/\mu_0$: (○) $2.5\times10^3$; (◇) $5\times10^3$; (▽) $10^4$; (□) $2.7\times10^4$; (▷) $6\times10^4$. Open symbols were obtained directly from Eq. (1), filled symbols with the support of computer simulations. Continuous lines have been added for the sake of clarity. The heavy horizontal line represents the boundary between continuous ($\tilde{c}>1$) and intermittent ($\tilde{c}<1$) DW motion regimes.

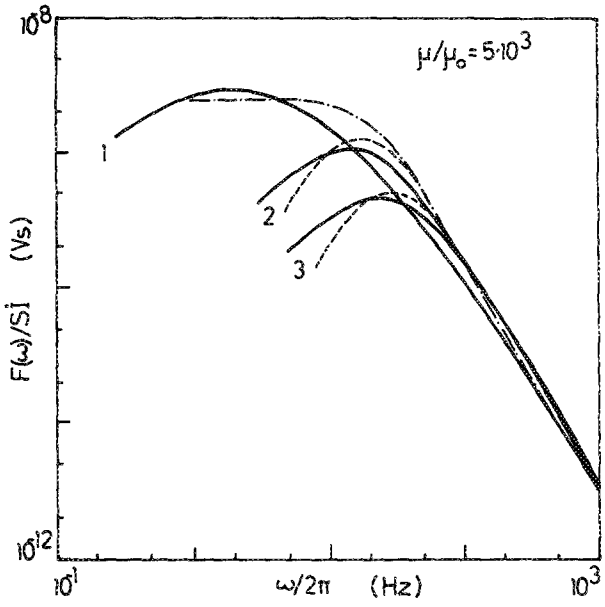


FIG. 7. Normalized $B$ noise power spectrum $F(\omega)/S\dot{I}$ vs analysis frequency $\omega/2\pi$ for fixed permeability $\mu/\mu_0=5\times10^3$ and variable $\dot{I}$: (1) $4.9\times10^{-3}$ T s$^{-1}$; (2) 0.15 T s$^{-1}$; (3) 0.49 T s$^{-1}$ (same as Figs. 3 and 4). Solid lines: experimental results. Broken-dotted line: prediction of computer simulations, assuming $A=1.65\times10^6$ A$^2$ m$^{-2}$ Wb$^{-1}$, $\xi=5.3\times10^{-9}$ Wb. Broken lines: predictions of Eq. (12), assuming $A=1.65\times10^6$ A$^2$ m$^{-2}$ Wb$^{-1}$ and (2) $\xi=6\times10^{-9}$ Wb; (3) $\xi=6.7\times10^{-9}$ Wb.

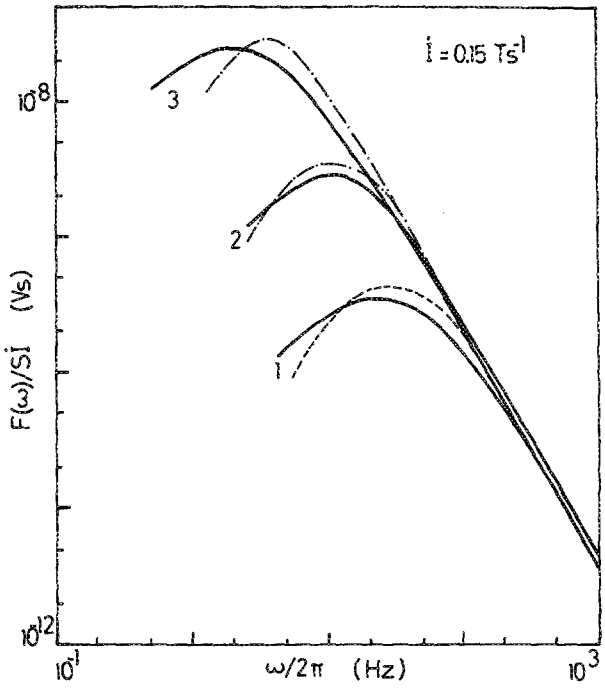


FIG. 8. Normalized $B$ noise power spectrum $F(\omega)/S\dot{I}$ vs analysis frequency $\omega/2\pi$ for fixed magnetization rate $\dot{I}=0.15$ T s$^{-1}$ and variable $\mu/\mu_0$: (1) $2.5\times10^3$; (2) $10^4$; (3) $6\times10^4$ (same as Fig. 5). Solid lines: experimental results. Broken line: prediction of Eq. (12), assuming $A=1.65\times10^6$ A$^2$ m$^{-2}$ Wb$^{-1}$, $\xi=5.5\times10^{-9}$ Wb. Broken-dotted lines: predictions of computer simulations, assuming $A=1.65\times10^6$ A$^2$ m$^{-2}$ Wb$^{-1}$ and (2) $\xi=8.4\times10^{-9}$ Wb; (3) $\xi=1.3\times10^{-8}$ Wb.

simple laws, even though a single analytical expression for $F(\omega)$, like Eq. (1) for $P_0$, could not be found. At high analysis frequencies ($\omega/2\pi\gtrsim1$ kHz), $F(\omega)$ is described by Eq. (3), where the parameter $k_F$ is independent of $\dot{I}$ and $\mu$, and is thus expected to be directly connected with the material microstructure. $k_F\simeq3.2\times10^{-10}$ V$^2$ T$^{-1}$ for the present experimental data. At lower $\omega$, the central characteristic of $F(\omega)$ is the presence of a maximum $F_M$ at a certain angular frequency $\omega_M$. The experimental dependence of $F_M$ and $\omega_M$ on $\dot{I}$ at various $\mu$ is shown in Figs. 9 and 10. $F_M$ is well described by Eq. (2), where the function $g_F(\dot{I})$ is fairly constant, $g_F(\dot{I})\simeq7.5\times10^{-12}$ V s, for $\dot{I}\lesssim10^{-2}$ T s$^{-1}$, and decreases when higher values of $\dot{I}$ are considered. The heavy line in Fig. 9 represents the condition $\tilde{c}=1$, as could be derived from the data of Fig. 6. It shows that the presence of $B$ clusters ($\tilde{c}<1$) corresponds to constant $g_F$, and the regime of continuous DW motion ($\tilde{c}>1$) to decreasing $g_F$. The fact that $F_M$ is proportional to $\dot{I}$ (constant $g_F$) when $\tilde{c}<1$ means that we are in the presence of $B$ clusters which do not change their average size, but only their time separation, when $\dot{I}$ is varied. When $\dot{I}$ is increased up to the point where $\tilde{c}\gtrsim1$, the $B$ clusters begin to coalesce, giving rise to a continuous signal and to a corresponding reduction of low-frequency fluctuations (decreasing $g_F$). As to $\omega_M$, Fig. 10 shows that its dependence on $\dot{I}$ is approximately $\omega_M\propto\dot{I}^{1/2}$, at least for values of $\dot{I}$ that are not too small. The dependence on $\mu$ is not so simple. To a first approximation, it can be described as $\omega_M\sim\mu^{-\alpha}$, where $\alpha$ lies somewhere in between $\frac{1}{2}$ and 1, de-

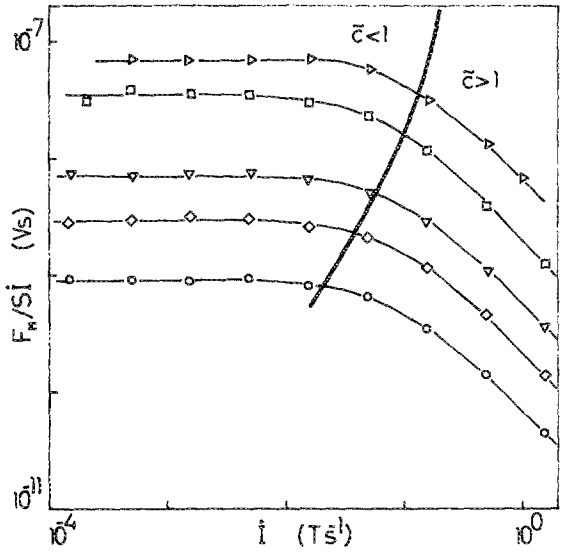


FIG. 9. Normalized maximum $F_M/S\dot{I}$ of $B$ noise power spectrum vs $\dot{I}$ for different values of $\mu/\mu_0$: (○) $2.5\times10^3$; (◇) $5\times10^3$; (▽) $10^4$; (□) $2.7\times10^4$; (▷) $6\times10^4$. Continuous lines have been added for the sake of clarity. The heavy line represents the boundary between continuous ($\tilde{c}>1$) and intermittent ($\tilde{c}<1$) DW motion regimes, as could be obtained from the data of Fig. 6.

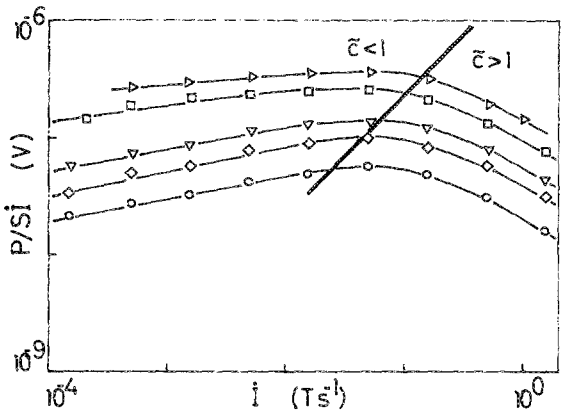


FIG. 11. Normalized $B$ noise power $P/S\dot{I}$ vs $\dot{I}$ for different permeabilities. For the meaning of symbols, heavy and continuous lines, see Fig. 9.

pending on $\dot{I}$ and $\mu$. Note, however, that the accuracy in the determination of $\omega_M$ is generally poor, and becomes even poorer at low $\dot{I}$ and high $\mu$, as $\omega_M$ approaches the lower bound of the $\omega$ range accessible to experiments.

A last parameter which can be used to characterize $F(\omega)$ is its area (the $B$ noise power) $P=\int F(\omega)d\omega/2\pi$, shown in Fig. 11. $P$ is approximately described by the law

$$P=S\dot{I}g_P(\dot{I})(\mu/\mu_0)^{1/2}. \tag{4}$$

The behavior of $g_P(\dot{I})$ is similar to that of the function $g_F(\dot{I})$ of Eq. (2). The main difference is that $g_P(\dot{I})$ is not a constant, but a weakly increasing function of $\dot{I}$, when $\dot{I}$ is low. This behavior reflects the fact that $F(\omega)$ for such values of $\dot{I}$ acquires a shape characterized by a slope in between $\omega^{-1}$ and $\omega^{-2}$ over a wide frequency range, as shown in Fig. 7.

We mentioned before that $F(\omega)$ can provide important information on clustering phenomena in BE. Other authors have pointed out the relationship between the spectrum cutoff frequency and the mean duration of $B$ clusters,[5,16] and have interpreted the presence of the maximum $F_M$ in terms of a time-amplitude correlation between subsequent $B$ clusters due to magnetostatic effects.[9] Our experiments show, however, that the maximum $F_M$ is even more pronounced in the regime $\tilde{c}>1$, where $B$ clusters are no longer present, so that a more general interpretation is needed. In the following section, this point will be discussed in the frame of the Langevin description of DW motion developed in paper I.

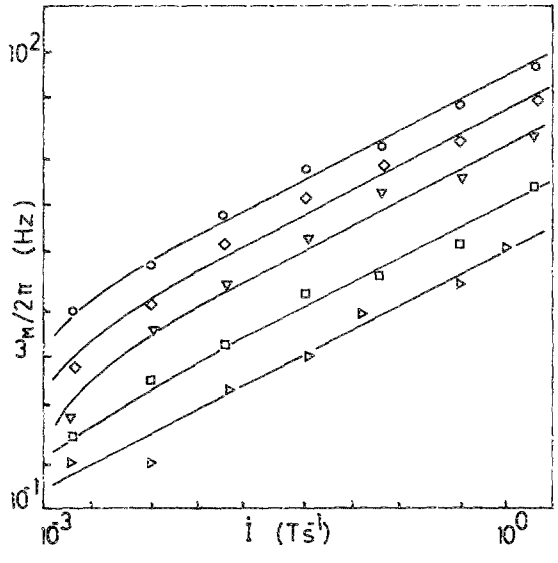


FIG. 10. Frequency $\omega_M/2\pi$ corresponding to the maximum $F_M$ of $B$ noise power spectrum vs $\dot{I}$ for different permeabilities. For the meaning of symbols and continuous lines, see Fig. 9.

## V. DISCUSSION

In this section, we shall apply the theory developed in paper I to the interpretation of the present experiments. We briefly recall that the theory is based on the following stochastic differential equation for the BE flux rate $\dot{\Phi}$:

$$\frac{d\dot{\Phi}}{dt}+\frac{\dot{\Phi}-S\dot{I}}{\tau}=-\frac{1}{\sigma G}\frac{dH_c}{dt}, \tag{5}$$

where $\sigma$ is the electrical conductivity ($\sigma=2\times10^6\ \Omega^{-1}\ \mathrm{m}^{-1}$ in the present case), $G=0.1356$, and

$$\tau=\sigma GS\mu. \tag{6}$$

The local coercive field $H_c$ obeys the Langevin equation

$$\frac{dH_c}{d\Phi}+\frac{H_c-\langle H_c\rangle}{\xi}=\frac{dW}{d\Phi}, \tag{7}$$

where the Wiener–Lévy process $W(\Phi)$ is characterized by

$$\langle|dW|^2\rangle=2A\,d\Phi. \tag{8}$$

The interaction of the moving DWs with the surrounding medium is described by the constant $A$ and the correlation length $\xi$, which are expected to be directly connected to the microstructure of the material under consideration. The theory predicts (after some approximations thoroughly discussed in paper I) that the amplitude probability distribu-

tion $P_0(\dot{\Phi})$ should precisely obey Eq. (1), with

$$\tilde{c} = S\dot{I}\,[(\sigma G)^2/A\,](1/\tau + 1/\tau_c) \tag{9}$$

and

$$\tau_c = \xi/S\dot{I}. \tag{10}$$

The power spectrum $F(\omega)$, on the other hand, is described by the equation

$$F(\omega) = 4S\dot{I}\frac{A}{(\sigma G)^2}\frac{\omega^2}{(\omega^2+\tau^{-2})(\omega^2+\tau_c^{-2})}. \tag{11}$$

Due to the approximations introduced in the analytical treatment, the behavior of $P_0(\dot{\Phi})$ and $F(\omega)$ predicted by Eqs. (5)–(8) tends to deviate from that of Eqs. (1) and (11) under some specific conditions (low $\dot{I}$ and/or high $\mu$). In these cases, improved predictions can be obtained by computer simulations[13] in which Eqs. (5)–(8) are used to numerically generate $\dot{\Phi}(t)$.

A first prediction of direct physical interest, implied by Eq. (11) but of general validity for any value of $\dot{I}$ or $\mu$, is that, at sufficiently high angular frequencies, the power spectrum approaches the law

$$F(\omega) \simeq 4S\dot{I}\,[A/(\sigma G)^2]/\omega^2. \tag{12}$$

Parameter $A$ describes the spatial fluctuations of short-range DW interactions and, as such, it is expected to be independent of $\dot{I}$ and $\mu$. We thus arrive at the conclusion that $F(\omega) \simeq k_F\dot{I}/\omega^2$, with $k_F$ independent of $\dot{I}$ and $\mu$. This is just what is found in experiments, as shown by Eq. (2). The experimental data are consistent with $A \simeq 1.65\times10^6$ $A^2\,m^{-2}\,Wb^{-1}$.

At lower $\omega$ values, the main feature predicted by Eq. (11) is the presence of a maximum

$$F_M = 4S\dot{I}\,[A/(\sigma G)^2](1/\tau + 1/\tau_c)^{-2}, \tag{13}$$

located at the frequency

$$\omega_M = (\tau\tau_c)^{-1/2}. \tag{14}$$

Even this prediction is in fair agreement with experiments. The broken lines in Figs. 7 and 8 represent the prediction of Eq. (11) when $A$ has the value given above and $\xi$ is conveniently adjusted. The main difference between the measured spectra and Eq. (11) is the shift of the predicted values of $\omega_M$ with respect to the experimental ones. This discrepancy is probably due to the oversimplified description of magnetostatic fields assumed in the theory. Recent studies[21] seem to indicate that it might be corrected by considering the details of the longitudinal flux propagation along the specimen.

A crucial aspect of the present comparison between theory and experiments is that the values of $A$ and $\xi$ obtained by fitting the spectrum $F(\omega)$ must also consistently determine $P_0(\dot{\Phi})$. Figures 5–8 show this to be in fact the case. A seemingly good agreement has been found in all cases, even when for high $\mu$ or low $\dot{I}$ Eqs. (1) and (11) are no longer good approximations of the theory. In these cases, $P_0(\dot{\Phi})$ and $F(\omega)$ were obtained numerically from computer simulations based on Eqs. (5)–(8), and, remarkably enough, a good and consistent agreement was still found, as shown by the broken dotted lines in Figs. 5 and 8. Note, in particular, that the computer simulations correctly reproduce the high $\dot{\Phi}$ decay of $P_0(\dot{\Phi})$ [more rapid than the one predicted by Eq. (1)] observed in experiments.

By this fitting procedure, the dependence of $\xi$ on $\dot{I}$ and $\mu$ consistent with the experimental data was obtained. This is shown in Fig. 12. The figure suggests that $\xi$ is independent of $\dot{I}$ and $\mu$, $\xi \simeq 5\times10^{-9}$ Wb, when $\tilde{c} < 1$, whereas $\xi$ is an increasing function of $\dot{I}$ and $\mu$ when $\tilde{c} > 1$. The dependence of $\xi$ on $\dot{I}$ can be interpreted, at least qualitatively, by considering, as discussed at the end of paper I, that $\xi \simeq n\,\xi_{DW}$, where $\xi_{DW}$ is the correlation length associated with the motion of a single DW, and $n$ is the number of simultaneously active DWs. $\xi_{DW}$, like $A$, is expected to be a constant, independent of $\dot{I}$ and $\mu$. When $\tilde{c} < 1$, the DW dynamics within a $B$ cluster is not affected by the rate of change of the applied field. This is confirmed by the fact that $F_M \propto \dot{I}$ in this regime. Under these conditions, $n$ is expected to be constant, $n \simeq n_0$, so that $\xi = n_0\,\xi_{DW}$, independent of $\dot{I}$. Conversely, when $\tilde{c} > 1$, the applied field forces more and more DWs to become active in order to provide the required total flux rate, so that $n$, and thus $\xi$, will gradually increase. The interpretation of the joint dependence of $\xi$ on $\dot{I}$ and $\mu$ does not seem so intuitive. It will be analyzed in detail in future papers.

## VI. CONCLUSION

In this paper we have tried to provide an experimental characterization of BE phenomenology amenable to a clear, direct physical interpretation. Basically, our approach has consisted in restricting $B$ noise measurements to the central part of the hysteresis loop, and in measuring the amplitude probability distribution $P_0(\dot{\Phi})$ and the power spectrum $F(\omega)$ under controlled values of the magnetization rate $\dot{I}$ and differential permeability $\mu$. Both $P_0(\dot{\Phi})$ and $F(\omega)$ have been found to obey remarkably simple and general laws [Eqs. (1)–(4)], which have been interpreted in the frame of the Langevin theory of DW motion developed in paper I. This theory seems to provide a consistent interpretation of the origin of BE. Its main weakness is, however, the fact that Eq. (7) is postulated, and not derived from a microscopic theory of coercivity, able to elucidate how the parameters $A$ and $\xi$ depend on $\dot{I}$, $\mu$, and the microstructural properties

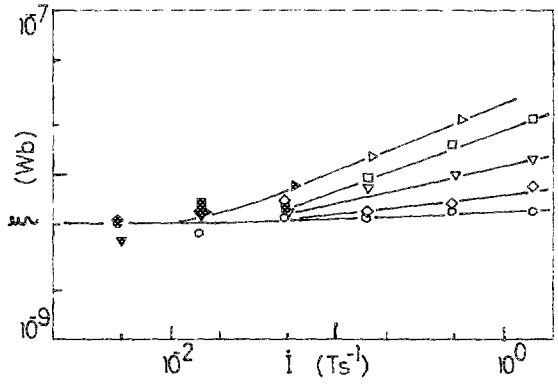


FIG. 12. Parameter $\xi$ of Eqs. (9)–(12) obtained by fitting experimental data vs $\dot{I}$ for different permeabilities. For the meaning of symbols and continuous lines, see Fig. 9. For the difference between open and filled in symbols, see Fig. 6.

(grain size, texture, internal and applied stresses, etc.) of a given material. This development would be of considerable importance, also in view of the general interest in BE as a nondestructive tool[5,19,20,22] to test the microstructural properties of magnetic materials.

## ACKNOWLEDGMENTS

This work was supported in part by the Progetto Finalizzato Energetica, under Grant CNR-ENEA, and by the Italian Ministry of Education.

[1] K. Stierstadt, *Der Magnetische Barkhausen Effekt*, *Springer Tracts in Modern Physics* (Springer, Berlin, 1966).
[2] H. Bittel, IEEE Trans. Magn. **MAG-5**, 359 (1969).
[3] G. Montalenti, Z. Angew. Phys. **28**, 295 (1970).
[4] J. C. McClure, Jr. and K. Schroder, CRC Crit. Rev. Solid State Sci. **6**, 45 (1976).
[5] S. Tiitto, Acta Polytech. Scand. **119**, 1 (1977).
[6] W. Grosse-Nobis, in *Noise in Physical Systems and 1/f Noise*, edited by P. H. E. Meijer, R. D. Mountain, and R. J. Soulen, Jr. (National Bureau of Standards, Washington, 1981), p. 317.
[7] B. Alessandro, C. Beatrice, G. Bertotti, and A. Montorsi, J. Appl. Phys. **64**, 5355 (1988).
[8] L. Storm, C. Heiden, and W. Grosse-Nobis, IEEE Trans. Magn. **MAG-2**, 434 (1966).
[9] M. Celasco, F. Fiorillo, and P. Mazzetti, Nuovo Cimento B **23**, 376 (1974).
[10] We employ SI units, with the convention $B = \mu_0 H + I$, and we assume that the term $\mu_0\, dH/dt$ can always be neglected with respect to $dI/dt$ in any flux rate evaluation. This implies that we can approximate the differential permeability $\mu \equiv dB/dH_a$ as $\mu \simeq dI/dH_a$.
[11] See G. Bertotti, F. Fiorillo, and M. P. Sassi, J. Magn. Magn. Mater. **23**, 136 (1981), and in *Noise in Physical Systems and 1/f Noise*, edited by P. H. E. Meijer, R. D. Mountain, and R. J. Soulen, Jr. (National Bureau of Standards, Washington, 1981), p. 324.
[12] Preliminary results on the present experiments have been reported in the following conference papers: B. Alessandro, G. Bertotti, and F. Fiorillo, Phys. Scr. **39**, 256 (1989); B. Alessandro, G. Bertotti, and A. Montorsi, J. Phys. (Paris) Colloq. **49**, C8-1907 (1988). See also Ref. 7.
[13] B. Alessandro, C. Beatrice, G. Bertotti, and A. Montorsi, J. Appl. Phys. **68**, 2901 (1990) (part I).
[14] G. Couderchon, J. L. Porteseil, G. Bertotti, F. Fiorillo, and G. P. Soardo, IEEE Trans. Magn. **MAG-25**, 3973 (1989).
[15] G. Bertotti, F. Fiorillo, and A. M. Rietto, IEEE Trans. Magn. **MAG-20**, 1481 (1984).
[16] P. Mazzetti and G. Montalenti, in *Proceedings of the ICM Conference*, Nottingham, 1964 (The Institute of Physics, London, 1964), p. 701.
[17] F. Fiorillo, in *Proceedings of the Soft Magnetic Material 7 Conference*, Blackpool, 1985 (University College, Cardiff, 1985), p. 99.
[18] V. M. Rudyak, Sov. Phys. Usp. **13**, 641 (1971).
[19] C. G. Gardner, G. A. Matzakanin, and D. L. Davidson, Int. J. Nondestruct. Test. **3**, 131 (1971).
[20] D. C. Jiles, IEEE Trans. Magn. **MAG-25**, 3455 (1989).
[21] G. Bertotti and F. Fiorillo, IEEE Trans. Magn. **MAG-25**, 3970 (1989).
[22] R. Rautioaho, P. Karjalainen, and M. Moilanen, J. Magn. Magn. Mater. **61**, 183 (1986).